Check for updates

Vortex fluidic enhanced enzymatic hydrolysis of gelatin from barramundi skin for 3D printing

Xiaoqi Sun[1†], Yixiao Wu[2†], Hao Wang[2†], Shan He[1,2,3,4]*,
David J. Young[5]*, Suresh Thennadil[2]*, Colin L. Raston [iD][3]*,
Mostafa R. Abukhadra[6], Ahmed M. El-Sherbeeny[7],
Shanggui Deng[1] and Matt Jellicoe[8]

[1]School of Food and Pharmacy, Zhejiang Ocean University, Zhoushan, Zhejiang, China, [2]Faculty of
Science and Technology, Charles Darwin University, Casuarina, NT, Australia, [3]College of Science and
Engineering, Flinders Institute for Nanoscale and Technology, Flinders University, Bedford Park, SA,
Australia, [4]BioNexus Pvt. Ltd, Adelaide, SA, Australia, [5]Glasgow College UESTC, University of Electronic
Science and Technology of China, Chengdu, China, [6]Materials Technologies and Their Applications
Lab, Faculty of Science, Beni-Suef University, Beni Suef, Egypt, [7]Department of Industrial Engineering,
College of Engineering, King Saud University, Riyadh, Saudi Arabia, [8]College of Medicine and Public
Health, Flinders University, Bedford Park, SA, Australia

Introduction: Processing with a continuous flow thin film vortex fluidic device (VFD) significantly improves the efficiency of enzymatic hydrolysis of barramundi skin gelatin compared with conventional methodology.

Methods: Degree of hydrolysis, scanning electron microscopy, rheological properties, texture profile analysis, and dynamic light scattering were applied in this study.

Results and discussion: The processing time was reduced from 120 min to 20 min, and the degree of hydrolysis increased from 55.0 to 74.5%. VFD-treated gelatin hydrolysates were combined with starch in different proportions for use as 3D printing inks. The ink composed of 60% starch and 40% fish gelatin hydrolyate gave an ink with a regular crosslinked internal structure, relatively high storage modulus (G'), adhesiveness (399 g.sec) and loss modulus (G") suitable for 3D printing. This new, one-step processing methodology has the potential to add value to an abundant waste product of the seafood industry.

1 Introduction

Fish processing co-products are fish material left over from the primary processing of fish manufacturing. The percentage of these co-products is around 50% of the starting material by weight (Abdollahi and Undeland, 2019), and imposes waste disposal cost in the absence of value-adding solutions. The Australian seafood industry, for example, discards over 150,000 tonnes of these co-products annually (Peter and Clive, 2006). Due to the high organic matter content, fish processing co-products are classified as a certified waste which is more costly to dispose of. Currently, it costs approximately AUD $150 per tonne to discard seafood waste (He et al., 2013), which means that the Australian seafood industry spends over AUD $15 million per annum on disposal of organic material that has potential for value-adding. This inefficient business model has been identified as not only cost-ineffective, but also environmentally harmful. Utilization of fish processing co-products is a high priority area for development within the global seafood industry.

Approximately 50% (w/w) of the dry weight of seafood waste is protein (Sasidharan and Venugopal, 2020). Of this fish protein, fish gelatin extracted from fish skin, could be a cost-effective source of gelatin, and is preferable to mammalian gelatin for people with particular cultural or religious dietary requirements (de la Caba et al., 2019). Gelatin hydrolysates, as a source of amino acids, are also easier for the body to absorb and digest due to their texture and better water-solubility (Nirmal et al., 2022).

3D Printing with food-grade materials offers novel, customized culinary products. Various edible materials can be used for 3D printing to create intricate food structures (Portanguen et al., 2019). Carbohydrate-based materials are popular in this respect, offering the opportunity to create structures that can be both visually appealing and have an interesting texture. Tanase-Opedal et al. (2019), for example, extracted lignin from forestry biomass, and used it to produce biocomposites with a 50% increase of antioxidant potential/cm^2. Portanguen et al. (2019) developed a 3D printed material based on starch and alginate to entrap nutrients, with a personalized shape to improve nutritional dietary intake by elderly consumers. However, there are several challenges for 3D printing with carbohydrates, such as limited structural integrity, susceptibility to moisture uptake, and lack of nutritional value (Alami et al., 2024). Liu et al. (2022) have suggested that mixing carbohydrate and protein could be the solution. 3D-Printed dietary fiber-rich snacks have been prepared using material derived from milk powder and rye flour (Guénard-Lampron et al., 2023). Fish gelatin has also been used for this purpose. Bian et al. (2024) mixed fish gelatin with gellan gum to make an edible ink for 3D printing. Fish gelatin mixed with carbohydrate would offer improved nutritional benefits than that for this latter composite.

The vortex fluidic device (VFD) (Figure 1) is a thin-film processing platform with a broad variety of research and commercial applications. The development of VFD processing technology resulted from research into the utilization and advancement of thin-film flow chemistry and thin-film microfluidics (Chen et al., 2014; Britton et al., 2017). VFD mixing overcomes problems with conventional batch processing by the induced intense micro-mixing associated with strong shear forces and high mass transfer (Britton et al., 2016). The processing capabilities of VFD mixing have rapidly expanded to small-molecule synthesis and drug delivery, as well as the manipulation of single-cell organisms (Britton et al., 2017). High rotational speeds can facilitate the formation of a dynamic thin film from the liquid inside the tube. Film thickness can be controlled by the rotational speed and liquid volume inside the tube (Solheim et al., 2019). An understanding of the fluid flow in the VFD has recently been developed (Alharbi et al., 2021; Matt et al., 2022). There is a "spinning top" or "typhoon like" topological flow ~1 mm in diameter, caused by the Coriolis force acting on the hemispherical base of the tube, in addition to double helical topological flow as Faraday wave eddies affected by the Coriolis force acting on the curved surface along the tube, which can be down to ~150 nm in diameter (Xu et al., 2019). The VFD can enhance chemical reaction rates and product selectivity. The rate of enzymatic reactions has been drastically increased, with a seven-fold acceleration on average for a range of transformations (Chuah et al., 2023). This phenomenon arises from a combination of Faraday pressure waves generated within the thin film, enhancing mass transport, and a collapse of the reaction transition state. Tethering enzymes to the tube's surface can facilitate the manufacture of complex small molecules in a single pass, while maintaining continuous flow (Britton et al., 2016). VFD processing has been used

to aid chemical reduction and elimination reactions, as well as material fabrication using the continuous flow mode of operation. For example, C_{60} has been assembled into cones, nanotubes, spicules and rods (Alharbi et al., 2021; Vimalanathan et al., 2017) without the use of surfactants or the need for additional downstream processing. The VFD technology is also efficient for mediating the production of diesters at room temperature (Britton et al., 2016) and enables multi-phase oxidation to occur without the need of use of phase transfer catalysts or organic solvents (Pye et al., 2018). VFD processing has been employed in food processing. He et al. (2020) encapsulated fish oil extracted from fish processing by-products using VFD processing, resulting in a smaller encapsulated particle sizes. Li et al. (2022) applied VFD processing to modify the internal structure of bacterial cellulose from kombucha production, resulting in an increased in crystallinity. However, the application of VFD on development of food 3D printing ink with different materials, including with fish gelatin, has not been reported yet.

The purpose of the present study was of the first time to investigate the impact of VFD treatment on fish gelatin hydrolysis and to explore the utility of the resulting hydrolylsate with starch to develop a 3D printing ink. This manuscript is of the first time that VFD technology has been used in 3D printing.

2 Materials and methods

2.1 Materials

Barramundi skin was purchased from a local fish market. All chemical materials of citric acid, NaOH, Alcalase and Formaldehyde were purchased from Sigma-Aldrich, Inc. (St. Louis, Missouri, United States).

2.2 Preparation of gelatin from barramundi skin

Gelatin was prepared according to a previously reported method with a slight modification (Nurilmala et al., 2020). The extraction was carried out by soaking the cut barramundi skin (approximately 1 × 1 cm) with 0.25% citric acid for 12 h at a skin and citric acid ratio of 1:4 (w/v). The skin was then washed with distilled water and extracted using vigorous agitation at 65°C for 7 h at a skin and distilled water ratio of 1:1 (w/v), followed by filtration through a calico and cotton cloth. The filtrate was dried using a vacuum evaporator at 60°C for 50 min.

2.3 Preparation of fish gelatin hydrolysates

The aforementioned prepared gelatin was hydrolyzed according to the procedure of Nurilmala et al. (2020) with a slight modification. The gelatin solution (6.67%, w/v) was adjusted to pH 8 with NaOH, and mixed with Alcalase (2%, v/v) (Sigma–Aldrich, St. Louis, MO, USA). For conventional hydrolysis, this mixture was treated at 55°C for 2 h during homogenization at 10,000 rpm. For the VFD-hydrolysis, this mixture was introduced to a VFD quartz tube (17.5 mm ID, 20 mm OD, 18.5 cm long) via jet feeds at a flow rate of 0.2 mL/min, rotation at 6000 rpm, and a tube inclination angle of 45°. This mixture was hydrolyzed at 55°C using a heating jacket. The retaining time of the liquid in the VFD quartz tube
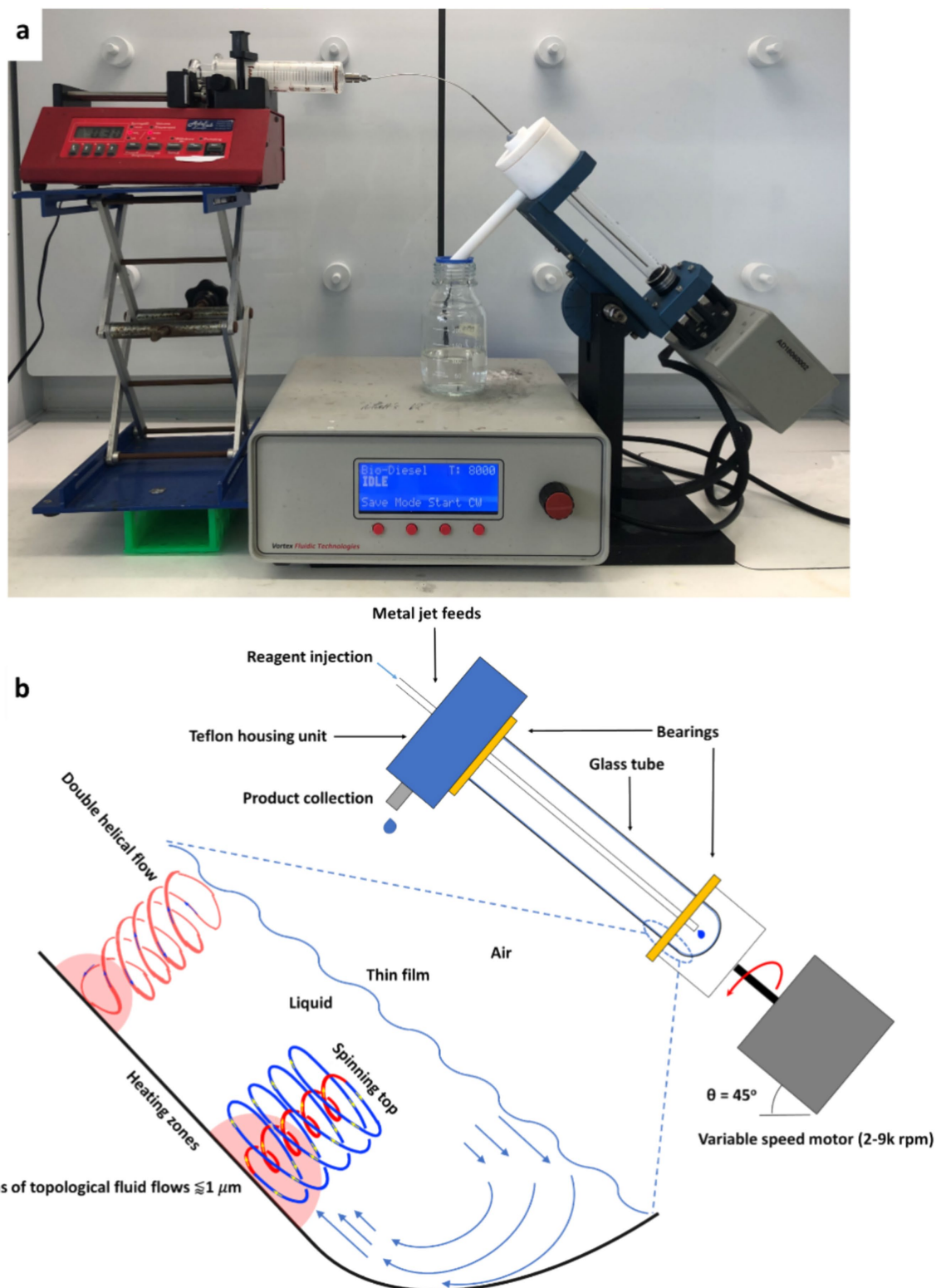
FIGURE 1
(A) The vortex fluidic device (VFD), (B) VFD operation and the high shear topological fluid flows in the thin film generated in the tube [Image credit: used with permission from a previous publication: "Sub-micron molding topological mass transport regimes in angled vortex fluidic flow," Alharbi et al. (2021); "High shear spheroidal topological fluid flow induced coating of polystyrene beads with C_{60} spicules," Jellicoe et al. (2021)].

was 20 min. In order of easy comparison, the difference of processing conditions between techniques of homogenization and VFD was presented in Table 1. Samples produced using these two processing techniques were then left at −20°C for 5 min to deactivate the enzyme. The solution was then centrifuged at 10,000 rpm at 4°C for 15 min, and the supernatant was obtained, and freeze-dried as gelatin hydrolysates.

TABLE 1 Different processing conditions between techniques of homogenization and VFD.

	Operational style	Processing speed	Processing time	Processing temperature
Homogenization	Stir liquid in a container	10,000 rpm	2 h	55°C
VFD	Rotate a quartz tube with liquid in	6,000 rpm	20 min	55°C

2.4 Determination of degree of hydrolysis (DH)

The degree of hydrolysis (DH) of these fish gelatin hydrolysates was measured using a formal titration method as described by Islam et al. (2021), with minor modifications. Briefly, 1.5 g of freeze-dried gelatin hydrolysate was dissolved in deionized water and the volume was made up to 50 mL. The solution was adjusted to pH 7.0 with 0.1 N NaOH, whereupon 10 mL of 38% (v/v) formaldehyde was added, and the solution was kept for 5 min at room temperature (25°C). Titration was conducted to the end point at pH 8.5 using standard 0.1 M NaOH, and the volume consumed was used to calculate the number of free amino groups (FAGs). The total nitrogen (TN) in the sample was determined by using the Kjeldahl method following the standard procedure (Bremner and Mulvaney, 1983). The FAGs and DH were calculated according to the following equations:

$$FAG_s\left(\%\right) = \left[\frac{V \times C \times \dfrac{14.007}{1000}}{S} \right] \times 100$$

$$DH\left(\%\right) = \left[\frac{\%FAG}{\%TN} \right] \times 100$$

Where V = mL of 0.1 M NaOH used; C = the concentration of sodium hydroxide used for titration (0.1 N); S = amount of sample (g); and TN = total nitrogen in the sample.

2.5 Scanning electron microscopy (SEM)

Samples were examined with a SEM (Inspect FEI F50 SEM (PS216)) at 5.0 kv and 2.0 m spot size. The processed liquid samples (20 µL) were drop cast onto a silicon substrate and air dried for 12 h. A 2 nm thick layer of platinum was then sputtered on top to avoid charging. Freeze-dried samples were submerged in liquid nitrogen for 2 min before being sliced into 5 mm x 5 mm x 2 mm cross sections prior to platinum sputtering.

2.6 Formulation of starch-fish gelatin hydrolysates for gelled 3D printing ink

The mixtures of gelatin hydrolysates and starch (CAS No.: 9005-25-8) were prepared to ensure gel formation essential for processing. A total of 7.7 grams of these combined components were dissolved in 50 mL of water at room temperature to initiate gelation. This gelation is critical for creating the stable structures needed in 3D printing applications. The resulting mixtures were formulated in varying proportions: 0% (0 g gelatin hydrolysates and 7.5 g starch), 20% (1.5 g gelatin and 6 g starch), 40% (3 g gelatin and 4.5 g starch), 60% (4.5 g gelatin and 3 g starch), and 80% (6 g gelatin and 1.5 g starch).

2.7 Rheological properties

The rheological properties of samples were determined according to La Gatta et al. (2021), using a Brookfield viscometer equipped with a thermo-container and programmable temperature controller (LV-III, HT-60, HT-110FR, respectively; Brookfield Engineering Laboratories, Inc.; Middleboro, MA, USA). The thermo-container was equipped with a sample chamber and a spindle (HT-2 and SC4-18 respectively; Brookfield Engineering Laboratories, Inc.; Middleboro, MA, USA). The system was cooled using a cooling plug assembly (HT-26Y, Brookfield Engineering Laboratories, Inc.; Middleboro, MA, USA) attached to a pressurized air nozzle. The temperature was controlled at 25°C, with a 4 mm gap setting, and 1.5 mL of each sample was dropped on to the plate. Viscosity profiles were measured using flow mode stepping as follows: The spindle was set with a shear rate from 0.01 to 500.00 rad.s^{-1} at 5 s intervals. For strain sweep, the shear frequency was controlled at 6.283 rad.s^{-1}. The strain sweep value was set to start at 1% and end at 10,000% for testing, with the final set up determined to be 1–5% to ensure the strain value range falling within linear viscoelstic regime. For the frequency sweep, the shear strain was set at 0.4 with the frequency value starting at 0.1 s^{-1} and ending at 10 s^{-1}.

2.8 Texture profile analysis

The sample size was 20 mm × 20 mm × 15 mm. Texture indicators, including hardness, adhesiveness, springiness, cohesiveness, gumminess, chewiness and resilience, were measured using a texture analyzer (TA.XTC-18, Baosheng, Shanghai, China) and a TA/36 cylindrical probe. The measurement speed was 2 mm/s, and the trigger force was 5 N. The compressive deformation of one sample was set to 60%. These eight texture indicators were derived from the TPA curves of each sample, and the TPA parameters listed above were calculated using Bourne's technique (Bourne, 2002).

2.9 3D printing

The 3D printing was performed with a syringe-type extrusion 3D printing system (Changxing Shiyin Technology Co. Ltd., Hangzhou, China). This 3D printing system consisted of an extrusion head with a heating barrel and pressure control to maintain the temperature and pressure of the formulation in the syringe and nozzle, respectively. The nozzle diameter was set to be 0.4 mm, the pressure was set to be 6 MPa, and the temperature was maintained at room temperature during 3D printing. The extrusion head was adjusted to move along the x, y, and z axes. The 3D modeling software Autodesk 123D design

(Autodesk, Inc., San Francisco, CA, USA) was used to design the 3D object (a cube with dimensions of $10 \times 10 \times 10$ mm) to be printed. Simplify3D slicer software (Simplify3D, Cincinnati, OH, USA) was used to set the printing conditions, including nozzle diameter, layer height, and extruder moving speed, and to slice the objects. The printing parameters used in this study are listed in Table 2. In order to present the 3D processing fidelity, A series of models in increasing complexity—1D, 2D, and 3D—to evaluate the printability and structural integrity of the hydrolysate-starch formulations. These models were chosen to systematically assess the hydrolysate's suitability for printing applications: 1D Model—A continuous straight line was printed as a basic test to assess the material's extrusion consistency and adhesion to the print platform; 2D Models—A square and a circle were selected for 2D printing to observe the material's layer cohesion and the ability to create smooth, continuous shapes without collapse or significant deformation; 3D Models—for a higher-fidelity test, a pyramid and a hollow cylinder was printed to evaluate the formulation's capability to maintain structural fidelity in more complex, layered geometries.

2.10 Dynamic light scattering (DLS)

As the preparation for DLS test, 0.1 g freeze-dried fish gelatin hydrolysates sample were dissolved in 2 mL MiliQ water in the ratio of 1:20 (w/v) in a 2 mL eppendorf tube. Vortex mixer (Malvern Panalytical Ltd., Malvern, WR14 1XZ, United Kingdom) was applied to shake the solution in eppendorf tube for 2 min to ensure samples to be fully dissolved. At ambient temperature, DLS (Nano ZS90, Malvern Instruments, Worcester, UK) was utilized to determine the particle size distribution of the encapsulated algal oil, equipped with a He-Ne 633 nm wavelength laser and a 173° detector angle. Depending on the particle sizes, the Malvern Zeta Sizer (Zetasizer Ultra, Malvern Panalytical Ltd., Malvern, WR14 1XZ, United Kingdom) was employed to measure the time-dependent variations of the light scattering.

2.11 Statistical analysis

Date represent the means + standard deviation of three replicates. They were analyzed by ANOVA. Least significant difference (LSD, 5%

TABLE 2 Three-dimensional (3D) printing parameters used in this study.

Processing parameter	Value
Heating barrel temperature	24°C
Nozzle temperature	24°C
Print platform temperature	24°C
Nozzle diameter	0.60 mm (0.84 mm for printing gum-mixture-based formulations)
Layer height	0.2 mm
Coasting distance	4 mm
Extruder moving speed	6 mm.s^{-1}

The authors have addressed most of the questions raised by the reviewers. I still have some additional comments.

level) was used to separate means when a significant p-value was obtained.

3 Results and discussion

3.1 Particle size distribution

Different samples of fish gelatin and gelatin hydrolysates were dispersed in water for dynamic light scattering (DLS) studies (Figure 2). The particle size of both gelatin hydrolysates after conventional treatment and VFD treatment were smaller than the original gelatin. However, despite only being processed for 20 min, the average particle size of gelatin hydrolysates resulting from VFD treatment (~200 nm) was much smaller than that obtained from conventional hydrolysis (~800 nm). This effect is presumably associated with the small higher shear topological fluid flows and associated local heating in liquids in the device (Figure 1B).

3.2 Micro-structures of fish gelatin before and after hydrolysis

The microstructure of fish gelatin before and after hydrolysis using the two different methods was determined using SEM (Figure 3). Uneven, mountain-range like topologies featured on the surface of the untreated gelatin (Figure 3A). This observation was consistent with previous studies of gelatin derived from tuna (Gómez-Guillén et al., 2007), tilapia (Weng and Zheng, 2015), and mackerel (Khiari et al., 2017). This uneven surface changed to flat with several indentations and holes after 120 min of conventional hydrolysis (Figure 3B). The number of these features increased after only 20 min VFD treatment (Figure 3C). This result is also consistent with enhanced hydrolysis associated with VFD treatment, as was the degree of hydrolysis (DH), 55.0 + 5.3% and 74.5 + 4.7% for fish gelatin hydrolysates produced from conventional method with processing time of 120 min and produced from VFD method with processing time of 20 min, respectively. The presence of holes in the VFD processed gelatin, Figure 3C is consistent with mixing down to submicron dimensions by the spinning top and double topological fluid flows (Alharbi et al., 2021; Matt et al., 2022). These topological fluid flows prevail at the operating processing parameters of the VFD, with the rotation speed at 6000 rpm and the tilt angle set at 45° which is optimal for most processing in the microfluidic platform. Enhanced enzymatic hydrolysis from VFD treatment has been reported previously. He et al. (2019) hydrolyzed milk protein using VFD processing and found that treatment for 20 min achieved smaller molecular weight milk protein hydrolysates than 2 h of processing using the conventional method. The fish gelatin hydrolsyates produced from VFD treatment were subsequently used for the 3D printing study.

3.3 Characterization of 3D printing inks made from starch and fish gelatin hydrolysates

Photographs of 3D printing inks made from different combination of starch and fish VFD gelatin hydrolysates are shown
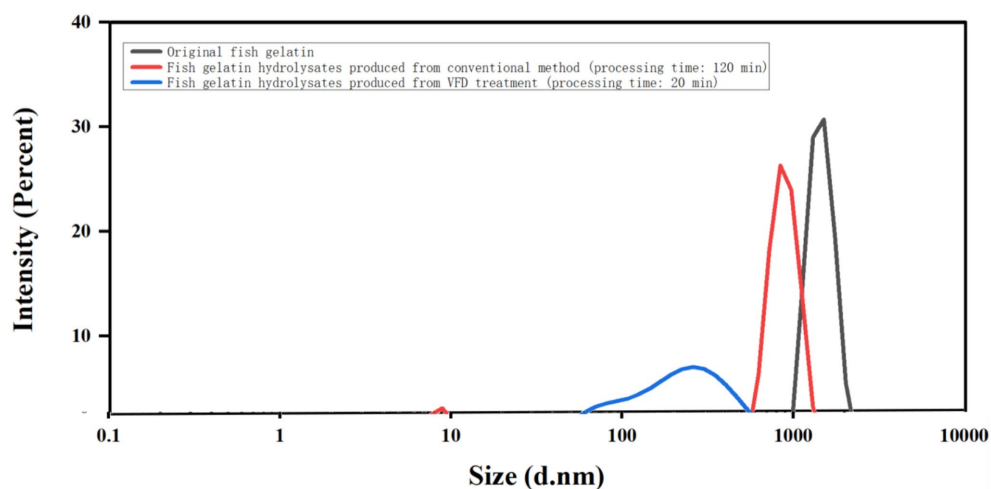
FIGURE 2
DLS data of the original fish gelatin, fish gelatin hydrolysates produced from conventional processing (time: 120 min), and fish gelatin hydrolysates produced from VFD processing (time: 20 min).
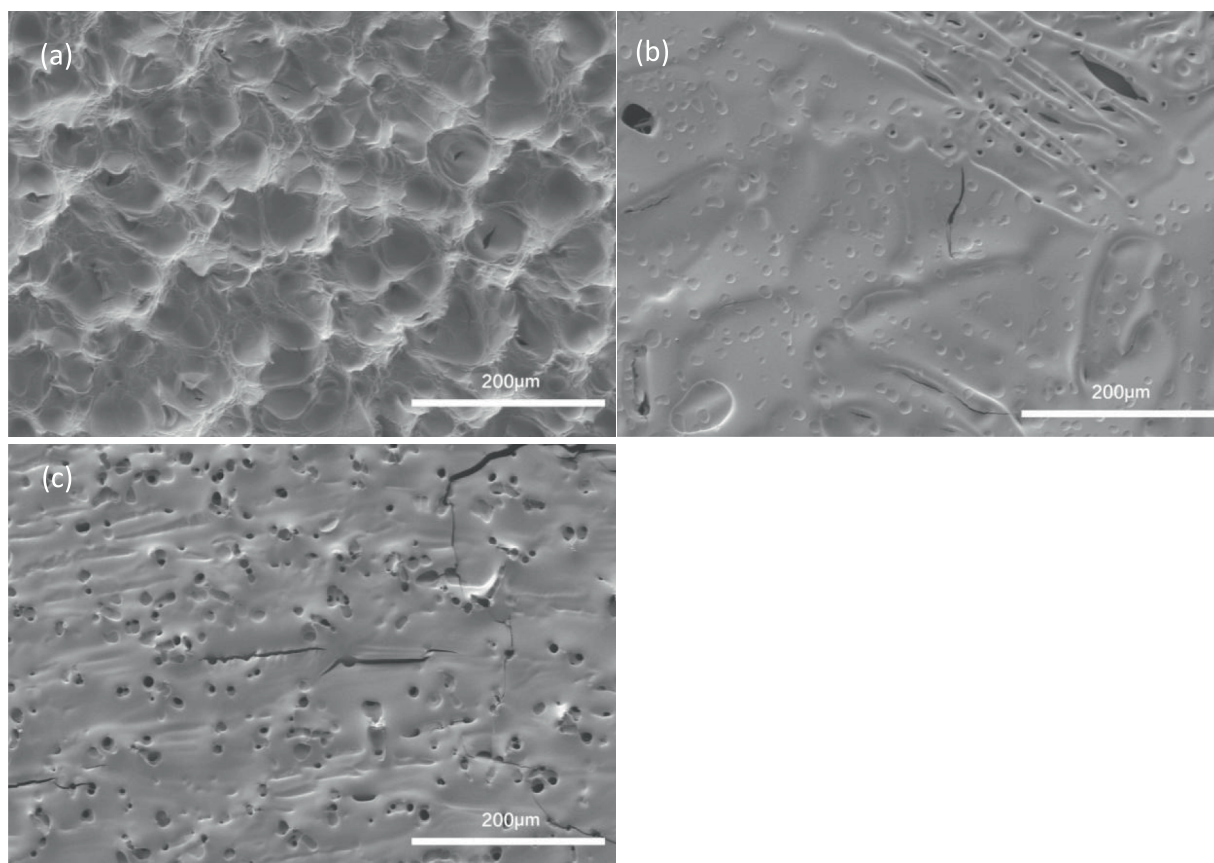

FIGURE 3
Scanning Electron Microscope images of (A) Original fish gelatin (B) Fish gelatin hydrolysates produced from conventional treatment (processing time: 120 min) (C) Fish gelatin hydrolysates produced from VFD treatment (processing time: 20 min).

in Figure 4. All samples gelled, which is a prerequisite for food 3D printing (Vancauwenberghe et al., 2017). The gel made from starch alone, however, was less stable (Figure 4A). This difference was further evidenced by differences in viscosity with increasing shear rate (Figure 5). A greater proportion of fish gelatin hydrolysate resulted in reduced viscosity and less change with increasing shear rate, although the 20% gelatin mixture had unusually low viscosity. This broad trend is consistent with increasing water-holding capacity

with high proportion of fish gel hydrolysate. The water-holding capacity of cod gelatin increased from 59.8 g/g sample to 70.4 g/g after hydrolysis by Flavorzyme (Zhang et al., 2022). Wu et al. (2018) also reported that salmon skin gelatine hydrolysates demonstrated strong water-holding capacity – even stronger than egg albumen and soybean protein, which are commonly used as commercial water binders in the food industry. This increased water-holding capacity of fish gelatin hydrolysates restrains water movement, therefore providing a better solid gel structure with reduced viscosity (Al-Nimry et al., 2021). The unusual low viscosity of the 20% gelatin mixture is caused by sub-optimal gel network formation: 20% of gelatin hydrolysates is not enough to form a cohesive gel network

FIGURE 4
Images of 3D printing inks. 100% starch +0% gelatin hydrolysates (A) 80% starch +20% gelatin hydrolysates (B) 60% starch +40% gelatin hydrolysates (C) 40% starch +60% gelatin hydrolysates (D) 20% starch +80% gelatin hydrolysates.

with the starch, leading to insufficient cross-linking. In the meantime, 20% of gelatine hydrolysates also interrupted the original gel formation of 100% pure starch. These double negative impacts resulted the network collapse more easily, leading to usual low viscosity (La Gatta et al., 2021). These measured viscosity are extremely high at low shear rates, even higher than mincemeat and mayonnaise (Pye et al., 2018). It was reported that the contribution of starch in 3D printing materials is to offer these materials Thixotropic Behavior, which means they exhibit high viscosities at low shear rates but become more fluid when shear is applied, the material's viscosity is responsive to shear. One typical example of this is during extrusion processing of 3D printing. Furthermore, comparing with standard 3D food printer being operated at pressures up to 0.5-1 MPa, the 3D printer applied in this study was operated at 6 MPa, which guaranteed the smooth 3D printing processing of all samples in this study. Indeed, there are several limitations for the operation of this high pressure 3D printer, such as increased energy consumption, high maintenance cost, and limited material compatibility. Further improvement of this high pressure printer is necessary to be carried out, though this high pressure 3D printer is sufficient for this current study.

The internal structure of each gel was studied by SEM (Figure 6). The starch-only gel formed an irregular network containing large, uneven gaps (Figure 6A). By comparison, the addition of 20% fish gelatin hydrolysate resulted in a more closely packed, more regular network (Figure 6B). Similar network ordering has been reported previously for a VFD-processed material, a tannic acid-gelatin network (Cao et al., 2021). The density of the network increased with increasing percentage of fish gelatin hydrolysate (Figures 6C–E). Gaps in the network were undetectable in the SEM image of gel made from 80% hydrolysate (Figure 6E).

FIGURE 5
Viscosity of 3D printing inks.
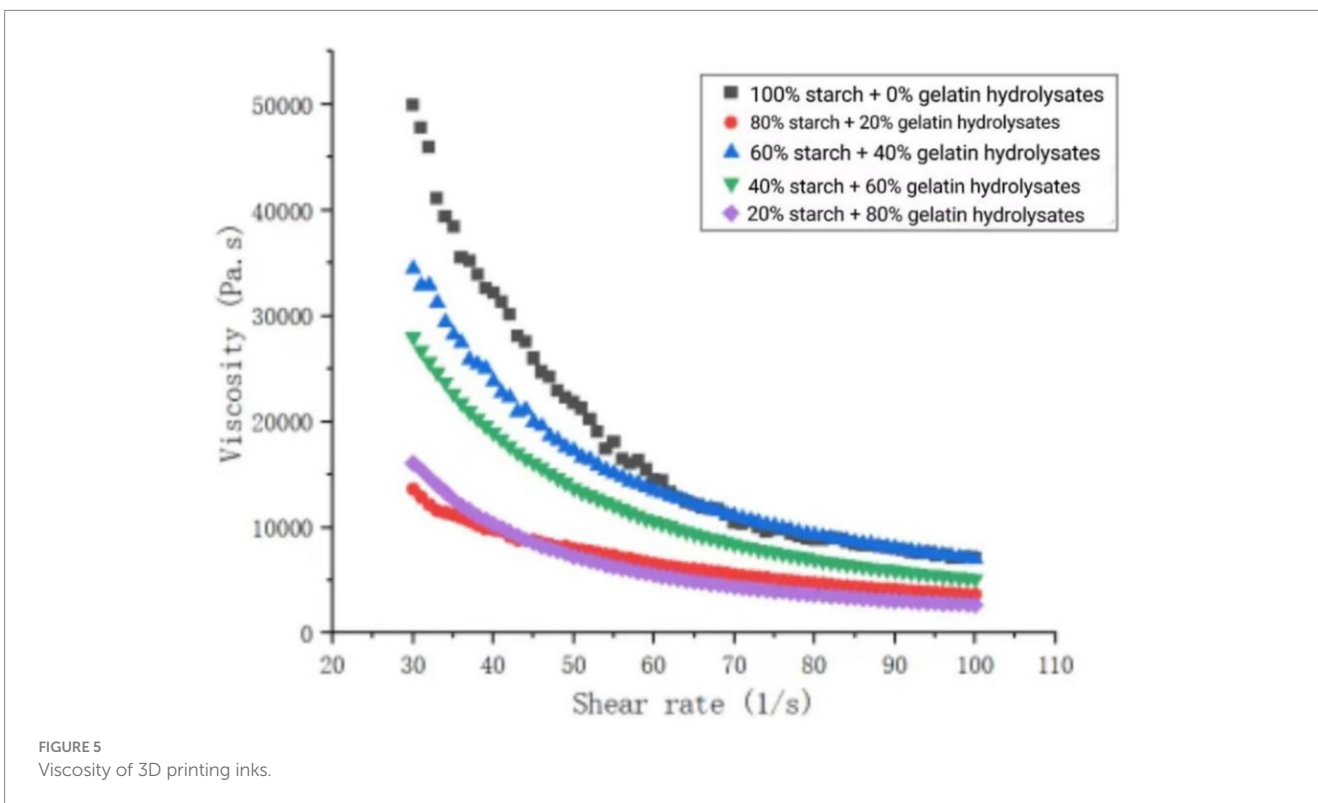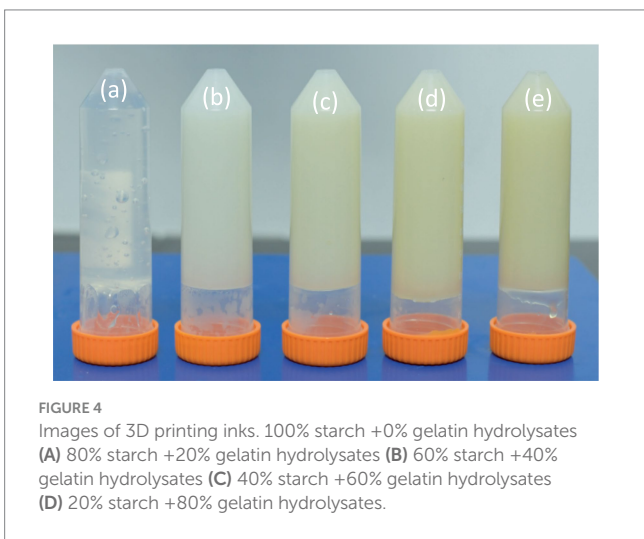
3.4 Rheological properties of 3D printing inks

The storage modulus G' (Figure 7A) and loss modulus G" (Figure 7B) versus the angular frequency with the strain sweep value from 1% to 10,000% for all samples were measured. In rheology, G' and G" are measured under a linear viscoelastic regime, which occurs at low strains. This ensures that the material response is linear, meaning that the relationship between stress and strain is proportional and does not involve non-linear deformations or structural breakdown. It was reported that Food 3D printing materials are at low strains as long as

they are able to be operated in the context of their 3D printer with extrusion model (Al-Nimry et al., 2021), which is the case of all developed 3D printing samples in this study. This ensured the accuracy of these rheological measurements. The 3D printing ink made from 60% starch and 40% gelatin hydrolysate showed the highest storage modules (G') and a more comparatively modest loss modulus (G"). The storage modulus (G') is associated with the elastic behavior of material. It measures the ability of the material to store elastic energy and return it when the applied stress is removed. A high G' suggests that the material can withstand deformation and stress without undergoing
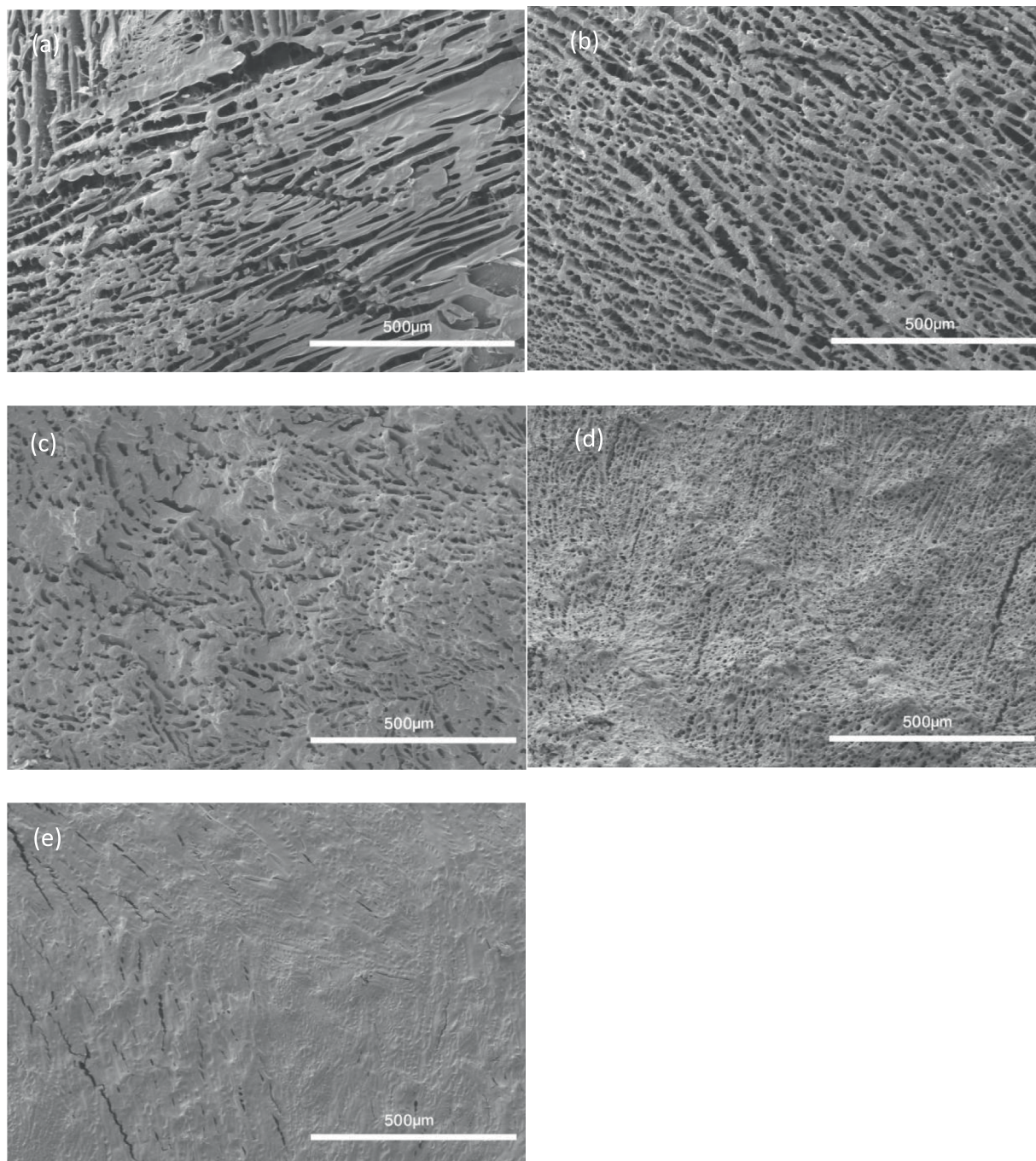
FIGURE 6
SEM images showing the internal structure of 3D printing inks. **(A)** 100% starch +0% gelatin hydrolysate **(B)** 80% starch +20% gelatin hydrolysate **(C)** 60% starch +40% gelatin hydrolysate **(D)** 40% starch +60% gelatin hydrolysate **(E)** 20% starch +80% gelatin hydrolysate.

significant permanent deformation (Werkmeister et al., 2001). This is beneficial for maintaining the shape fidelity of the printed layers. A high G' not only helps prevent excessive deformation or sagging of the printed structure during the printing process, but also allows for faster printing speeds since the material can recover its shape quickly after extraction (Li et al., 2021). It has been reported previously that the closer to even proportion of starch and gelatin hydrolysates resulted in the best synergistic interaction of these 2 materials. Starch contributes to the gel network's bulk and stiffness while gelatin hydrolsyates enhance flexibility and water retention. The closer 1:1 ratio of gelatin hydrolysates concentration is ideal for forming a well-distributed hydrocolloid network within the starch matrix, reinforcing elasticity without overloading the system with excessive water-binding that could weaken the gel (Donmez et al., 2021). This previous report is in alignment with the result of Figure 7A in this study. The G' value positively correlates with adhesiveness for 3D printing ink (Zheng et al., 2021). This was evident in the texture profile analysis (Figure 8) in which the 3D printing ink made from 60% starch and 40% gelatin hydrolysates demonstrated the best adhesiveness. A 3D printing

material with low G' leads to poor layer adhesion. Indeed, Figures 7A,B demonstrated decrease of G' and G" with increase of frequency, respectively. This might indicates the change of samples due to fracture. But the drops in storage modulus (G') in Figure 7A and loss modulus (G") in Figure 7B indicate minor reductions in the elasticity and viscosity of the samples, respectively. Therefore, despite these reductions, the samples can still be 3D printed smoothly without fracture due to the balanced viscoelastic properties within an optimal range for 3D printing. The balance between G' and G" is crucial for maintaining printability. The high enough G' allows the printed material to retain its shape and resist deformation under stress, which is essential for layer-by-layer construction. Simultaneously, a moderate G" ensures the ink has adequate viscosity to flow through the nozzle smoothly without causing blockages or fractures.

Different letters in the same graph indicate a significant difference ($p < 0.05$) according to one-way ANOVA and LSD test.

Loss modulus (G") is associated with the viscous behavior of a material. A moderate, rather than high G," is desirable for 3D printing ink. It provides a degree of viscosity during the printing process (Kyle
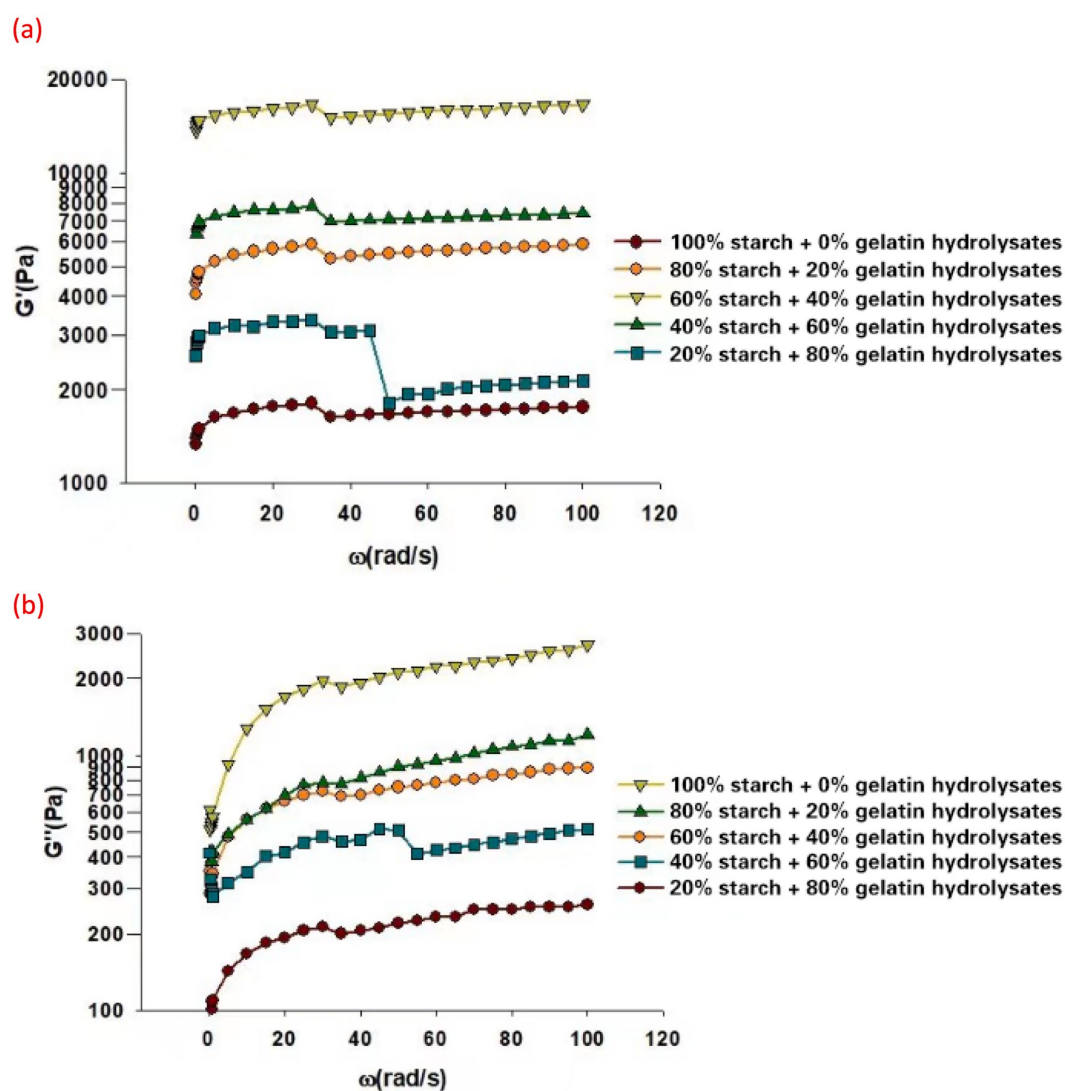
FIGURE 7
Rheological properties of 3D printing inks. **(A)** Storage modulus (G') **(B)**. Loss modulus (G").

et al., 2017). This can help in achieve better layer adhesion and a smooth deposition of the ink, contributing to overall printing quality. A 3D printing ink with excessively high G" may be too viscous, making it challenging to extrude through the 3D printer nozzle.

3.5 Printability of 3D printing inks made from different combination of starch and fish gelatin hydrolysates

The ideal 3D printing ink should have a balanced combination of high G' and moderate G" to facilitate layer-by-layer printing. A high G' value, particularly when G' is significantly greater than G," indeed indicates that the material exhibits solid-like, elastic

characteristics, which is desirable for 3D printing as it helps the ink maintain shape upon extrusion (Chuah et al., 2023). However, rigidity in 3D printing context should not be interpreted as an overly firm or brittle structure. Instead, an ideal 3D printing ink requires a balance—where G'> > G" supports form retention, but with sufficient viscoelasticity represented by G" to allow smooth flow through the nozzle and good layer adhesion (Gómez-Guillén et al., 2007). The 3D-printing ink made from 60% starch and 40% fish gelatin hydrolysates appeared to have the best balance of these parameters. Its moderate G" values allowed the hydrolysate-starch inks to retain enough flexibility to extrude and adhere between layers while providing the necessary elasticity to form and maintain complex shapes. In other words, while the ratio of G' to G" (G'> > G") implies a dominance of elastic properties, it does not

FIGURE 8
Texture profile analysis of 3D printing inks.
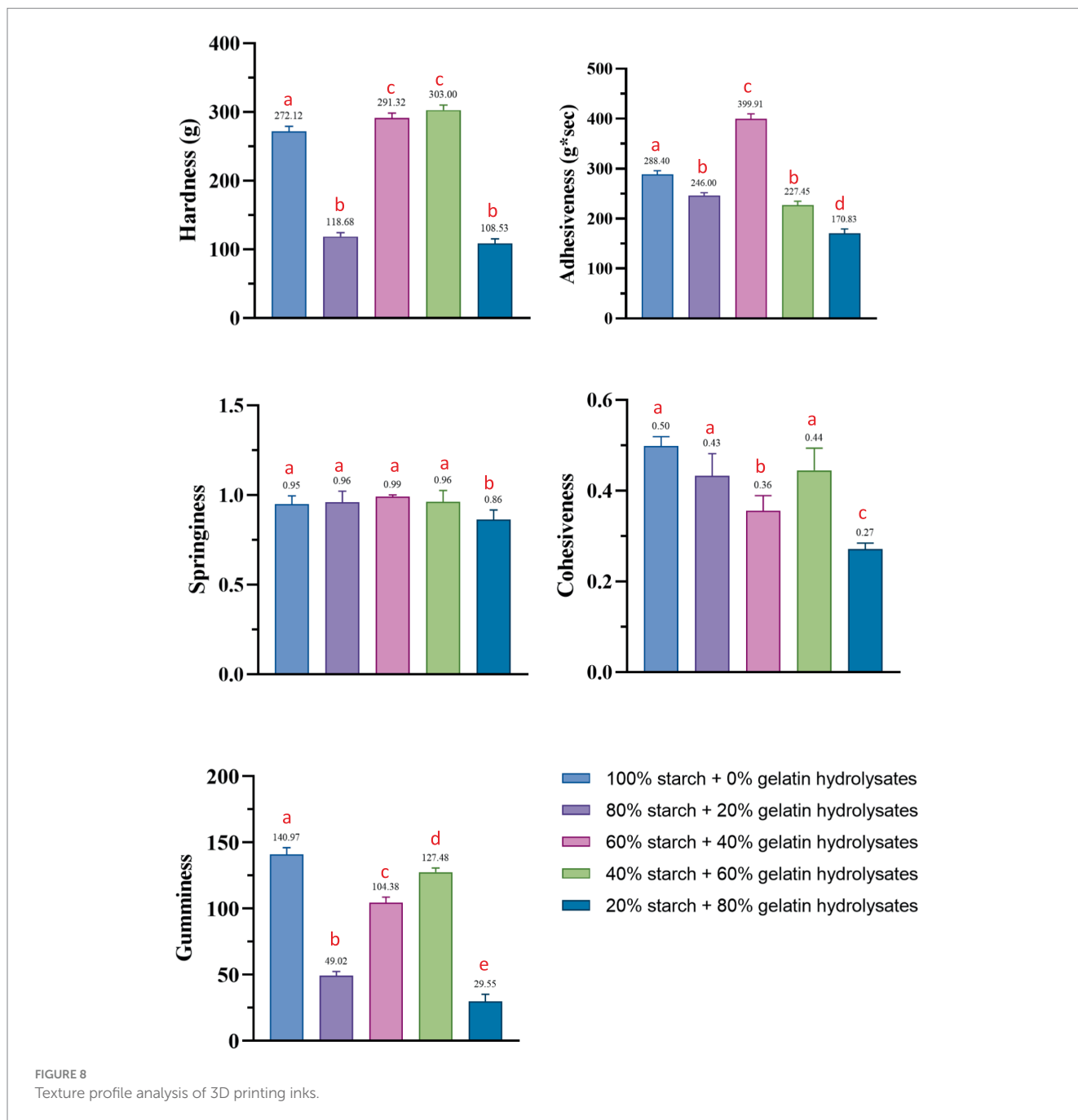
indicate a rigid structure unsuitable for extrusion, but rather an optimal viscoelastic balance essential for food 3D printing applications (Guénard-Lampron et al., 2023). This prediction was validated by comparing the outcome of using each ink for 3D printing. 1D, 2D, and 3D shapes (cylinders and pyramids) were printed for 3D printing inks to assess their fidelity in this study (Figure 9). The printing using 60% starch and 40% gelatin hydrolysate exhibited the best printing accuracy. The 3D-printing
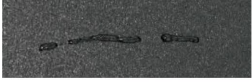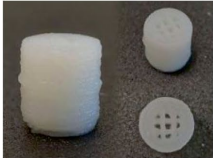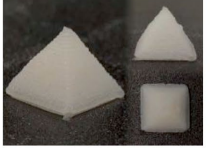
	1D images	2D images	3D images
100% starch+0% gelatin hydrolysates			
80% starch+20% gelatin hydrolysates			
60% startch+40% hydrolysates			
40% starch+60% hydrolysates			
20% starch+80% hydrolysates			

FIGURE 9
1D-, 2D-, and 3D-printing images using inks from different combination of starch and fish gelatin hydrolysates.

ink made from 80% starch and 20% gelatin hydrolysate could not produce the intended 2D-printing image due to its low G' value. The 3D-printing ink made from 100% starch could not produce even a 1D-printing image, due to its the lowest G' value indicating the lowest elasticity, and high G" value. Therefore, they were excluded from the 3D-printing trial. Our previous studies have presented the advantages of applying VFD on encapsulation of fish oil extracted from fish viscera with smaller particle size (Shan et al., 2019), and enzymatic hydrolyzation of protein extracted from fish filet with shorter processing (He et al., 2019). This study further enriched the knowledge of application of VFD on value-adding various fish processing waste components, demonstrating the advantage of sustainability of VFD technology on seafood processing industry.

4 Conclusion

This study compared conventional enzymatic hydrolysis of barramundi fish skin gelatin with hydrolysis using continuous flow thin film vortex fluidic device (VFD) processing. The latter technique gave greater hydrolysis in a quarter of the processing time. Combining the VFD hydrolyzed fish gelatin with starch produced inks that could be used for accurate 3D printing. The internal structure, rheology and texture of these 3D-printing inks were analyzed, and these parameters correlated with the superior 3D-printing ink made from 60% starch and 40% fish gelatin hydrolyate, which possessed the most regular cross-linked internal structure, highest storage modulus (G'), adhesiveness (399.0 g.sec) and a modest loss modulus (G"). This study has developed a new one-step method to increase the efficiency of enzymatic hydrolysis of seafood waste which can be combined with starch to give a good quality 3D-printing ink suitable for use in the food industry.

Data availability statement

The raw data supporting the conclusions of this article will be made available by the authors, without undue reservation.

Author contributions

Funding

Conflict of interest

SH was employed by the BioNexus Pvt. Ltd.

The remaining authors declare that the research was conducted in the absence of any commercial or financial relationships that could be construed as a potential conflict of interest.

Publisher's note

References

Abdollahi, M., and Undeland, I. (2019). Physicochemical and gel-forming properties of protein isolated from salmon, cod and herring by-products using the pH-shift method. *Food Sci. Technol.* 101, 678–684. doi: 10.1016/j.lwt.2018.11.087

Alami, A. H., Olabi, A. G., Khuri, S., Aljaghoub, H., Alasad, S., Ramadan, M., et al. (2024). 3D printing in the food industry: recent progress and role in achieving sustainable development goals. *Ain Shams Eng. J.* 15:102386. doi: 10.1016/j.asej.2023.102386

Alharbi, T. M. D., Jellicoe, M., Luo, X., Vimalanathan, K., Alsulami, I. K., Al Harbi, B. S., et al. (2021). Sub-micron moulding topological mass transport regimes in angled vortex fluidic flow. *Nanoscale Adv.* 3, 3064–3075. doi: 10.1039/d1na00195g

Al-Nimry, S., Dayah, A. A., Hasan, I., and Daghmash, R. (2021). Cosmetic, biomedical and pharmaceutical applications of fish gelatin/hydrolysates. *Mar. Drugs* 19:145. doi: 10.3390/md19030145

Bian, M., Jiang, S., Liu, S., Zhang, L., Miao, S., Zhou, F., et al. (2024). Fish gelatin and gellan gum mixture as edible ink for 3D printing. *J. Food Eng.* 362:111762. doi: 10.1016/j.jfoodeng.2023.111762

Bourne, M. C. (2002). Food texture and viscosity concept and measurement. *2nd* Edn. New York, NY: Academic Press.

Bremner, J. M., and Mulvaney, C. S. (1983). Nitrogen—total. *Methods Soil Anal. Part 2 Chem. Microbiol. Properties* 9, 595–624.

Britton, J., Dalziel, S. B., and Raston, C. L. (2016). The synthesis of dicarboxylate esters using continuous flow vortex fluidics. *Green Chem.* 18, 2193–2200. doi: 10.1039/C5GC02494C

Britton, J., Meneghini, L. M., Raston, C. L., and Weiss, G. A. (2016). Accelerating enzymatic catalysis using Vortex fluidics. *Angew. Chem. Int. Ed. Engl.* 55, 11387–11391. doi: 10.1002/anie.201604014

Britton, J., Stubbs, K. A., Weiss, G. A., and Raston, C. L. (2017). Vortex fluidic chemical transformations. *Chem. Eur. J.* 23, 13270–13278. doi: 10.1002/chem.201700888

Cao, X., Joseph, N., Jellicoe, M., Al-Antaki, A. H. M., Luo, X., Su, D., et al. (2021). Vortex fluidics mediated non-covalent physical entanglement of tannic acid and gelatin for entrapment of nutrients. *Food Funct.* 12, 1087–1096. doi: 10.1039/D0FO02230F

Chen, X., Smith, N. M., Iyer, K. S., and Raston, C. L. (2014). Controlling nanomaterial synthesis, chemical reactions and self assembly in dynamic thin films. *Chem. Soc. Rev.* 43, 1387–1399. doi: 10.1039/C3CS60247H

Chuah, C., Lou, X., Tavakoli, J., Tang, Y., and Raston, C. (2023). Thin-film flow technology in controlling the organization of materials and their properties. *Aggregate* 5:e433. doi: 10.1002/agt2.433

de la Caba, K., Guerrero, P., Trung, T. S., Cruz-Romero, M., Kerry, J. P., Fluhr, J., et al. (2019). From seafood waste to active seafood packaging: an emerging opportunity of the circular economy. *J. Clean. Prod.* 208, 86–98. doi: 10.1016/j.jclepro.2018.09.164

Donmez, D., Pinho, L., Patel, B., and Campanella, P. (2021). Characterization of starch–water interactions and their effects on two key functional properties: starch gelatinization and retrogradation. *Curr. Opin. Food Sci.* 39, 103–109. doi: 10.1016/j.cofs.2020.12.018

Gómez-Guillén, M. C., Ihl, M., Bifani, V., Silva, A., and Montero, P. (2007). Edible films made from tuna-fish gelatin with antioxidant extracts of two different murta ecotypes leaves (*Ugni molinae* Turcz). *Food Hydrocoll.* 21, 1133–1143. doi: 10.1016/j.foodhyd.2006.08.006

Guénard-Lampron, V., Liu, X., Masson, M., and Blumenthal, D. (2023). Screening of different flours for 3D food printing: optimization of thermomechanical process of soy and rye flour dough. *Innovative Food Sci. Emerg. Technol.* 87:103394. doi: 10.1016/j.ifset.2023.103394

He, S., Franco, C., and Zhang, W. (2013). Functions, applications and production of protein hydrolysates from fish processing co-products (FPCP). *Food Res. Int.* 50, 289–297. doi: 10.1016/j.foodres.2012.10.031

He, S., Joseph, N., Luo, X., and Raston, C. L. (2019). Vortex fluidic mediated food processing. *PLoS One* 14:e0216816. doi: 10.1371/journal.pone.0216816

He, S., Joseph, N., Mirzamani, M., Pye, S. J., Al-anataki, A. H. M., Whitten, A. E., et al. (2020). Vortex fluidic mediated encapsulation of functional fish oil featuring in situ probed small angle neutron scattering. *NPJ Sci. Food* 4:12. doi: 10.1038/s41538-020-00072-1

Islam, M. S., Hongxin, W., Admassu, H., Noman, A., Ma, C., and An Wei, F. (2021). Degree of hydrolysis, functional and antioxidant properties of protein hydrolysates from grass turtle (*Chinemys reevesii*) as influenced by enzymatic hydrolysis conditions. *Food Sci. Nutr.* 9, 4031–4047. doi: 10.1002/fsn3.1903

Jellicoe, M., Vimalanathan, K., Gascooke, J., Raston, C. L., and Raston, C. L. (2021). High shear spheroidal topological fluid flow induced coating of polystyrene beads with C60 spicules. *Chem. Commun.* 57, 5638–5641. doi: 10.1039/D0CC07165J

Khiari, Z., Rico, D., Martin-Diana, A. B., and Barry-Ryan, C. (2017). Valorization of fish by-products: rheological, textural and microstructural properties of mackerel skin gelatins. *J. Mat. Cycles Waste Manage.* 19, 180–191. doi: 10.1007/s10163-015-0399-2

Kyle, S., Jessop, Z. M., Al-Sabah, A., and Whitaker, I. S. (2017). Printability'of candidate biomaterials for extrusion based 3D printing: state-of-the-art. *Adv. Healthc. Mater.* 6:1700264. doi: 10.1002/adhm.201700264

La Gatta, A., Tirino, V., Cammarota, M., La Noce, M., Stellavato, A., Pirozzi, A. V. A., et al. (2021). Gelatin-biofermentative unsulfated glycosaminoglycans semi-interpenetrating hydrogels via microbial-transglutaminase crosslinking enhance osteogenic potential of dental pulp stem cells. *Regener. Biomat.* 8:rbaa052. doi: 10.1093/rb/rbaa052

Li, S., Jellicoe, M., Luo, X., Igder, A., Campbell, J. A., Tian, B., et al. (2022). Continuous flow vortex fluidic transformation of kombucha cellulose into more compact and crystalline fibers br. *ACS Sustain. Chem. Eng.* 10, 4279–4288. doi: 10.1021/acssuschemeng.2c00208

Li, N., Qiao, D., Zhao, S., Lin, Q., Zhang, B., and Xie, F. (2021). 3D printing to innovate biopolymer materials for demanding applications: a review. *Mater. Today Chem.* 20:100459. doi: 10.1016/j.mtchem.2021.100459

Liu, Z., Xing, X., Xu, D., Chitrakar, B., Hu, L., Hati, S., et al. (2022). Correlating rheology with 3D printing performance based on thermo-responsive κ-carrageenan/Pleurotus ostreatus protein with regard to interaction mechanism. *Food Hydrocoll.* 131:107813. doi: 10.1016/j.foodhyd.2022.107813

Matt, J., Agil, I., Clarence, C., Darryl, B. J., Xuan, L., Keith, A. S., et al. (2022). Vortex fluidic induced mass transfer across immiscible phases. *Chem. Sci.* 13, 3375–3385. doi: 10.1039/D1SC05829K

Nirmal, N. P, Santivarangkna, C., Rajput, M. S., Benjakul, S., and Maqsood, S. (2022). Valorization of fish byproducts: sources to end-product applications of bioactive protein hydrolysate. *Compr. Rev. Food Sci. Food Saf.* 21, 1803–1842. doi: 10.1111/1541-4337.12917

Nurilmala, M., Hizbullah, H. H., Karnia, E., Kusumaningtyas, E., and Ochiai, Y. (2020). Characterization and antioxidant activity of collagen, gelatin, and the derived peptides from yellowfin tuna (*Thunnus albacares*). *Skin. Marine Drugs* 18:98-. doi: 10.3390/md18020098

Peter, D., and Clive, H. (2006). An overview of the Australian seafood industry. Published online. Available at: http://aaa.ccpit.org/Category7/mAttachment/2006/Dec/13/asset000070002007202file1.pdf (Accessed December 13, 2006).

Portanguen, S., Tournayre, P., Sicard, J., Astruc, T., and Mirade, P.-S. (2019). Toward the design of functional foods and biobased products by 3D printing: a review. *Trends Food Sci. Technol.* 86, 188–198. doi: 10.1016/j.tifs.2019.02.023

Pye, S. J., Dalgarno, S. J., Chalker, J. M., and Raston, C. L. (2018). Organic oxidations promoted in vortex driven thin films under continuous flow. *Green Chem.* 20, 118–124. doi: 10.1039/C7GC03352D

Sasidharan, A., and Venugopal, V. (2020). Proteins and co-products from seafood processing discards: their recovery, functional properties and applications. *Waste Biomass Valorization* 11, 5647–5663. doi: 10.1007/s12649-019-00812-9

Shan, H., Nikita, J., Xuan, L., and Colin, R. (2019). Continuous flow thin film microfluidic mediated nano-encapsulation of fish oil. *LWT* 103, 88–93. doi: 10.1016/j.lwt.2018.12.066

Solheim, T. E., Salvemini, F., Dalziel, S. B., and Raston, C. L. (2019). Neutron imaging and modelling inclined vortex driven thin films. *Sci. Rep.* 9:2817. doi: 10.1038/s41598-019-39307-x

Tanase-Opedal, M., Espinosa, E., Rodríguez, A., and Chinga-Carrasco, G. (2019). Lignin: a biopolymer from forestry biomass for biocomposites and 3D printing. *Materials* 12:3006. doi: 10.3390/ma12183006

Vancauwenberghe, V., Katalagarianakis, L., Wang, Z., Meerts, M., Hertog, M., Verboven, P., et al. (2017). Pectin based food-ink formulations for 3-D printing of customizable porous food simulants. *Innovative Food Sci. Emerg. Technol.* 42, 138–150. doi: 10.1016/j.ifset.2017.06.011

Vimalanathan, K., Shrestha, R. G., Zhang, Z., Zou, J., Nakayama, T., and Raston, C. L. (2017). Surfactant-free fabrication of fullerene C60 Nanotubules under shear. *Angew. Chem. Int. Ed.* 56, 8398–8401. doi: 10.1002/anie.201608673

Weng, W., and Zheng, H. (2015). Effect of transglutaminase on properties of tilapia scale gelatin films incorporated with soy protein isolate. *Food Chem.* 169, 255–260. doi: 10.1016/j.foodchem.2014.08.012

Werkmeister, S., Dawson, A. R., and Wellner, F. (2001). Permanent deformation behavior of granular materials and the shakedown concept. *Transp. Res. Rec.* 1757, 75–81. doi: 10.3141/1757-09

Wu, R., Wu, C., Liu, D., Yang, X., Huang, J., Zhang, J., et al. (2018). Antioxidant and anti-freezing peptides from salmon collagen hydrolysate prepared by bacterial extracellular protease. *Food Chem.* 248, 346–352. doi: 10.1016/j.foodchem.2017.12.035

Xu, J., Xia, R., Zheng, L., Yuan, T., and Sun, R. (2019). Plasticized hemicelluloses/chitosan-based edible films reinforced by cellulose nanofiber with enhanced mechanical properties. *Carbohydr. Polym.* 224:115164. doi: 10.1016/j.carbpol.2019.115164

Zhang, H., Zhang, Y., Javed, M., Cheng, M., Xiong, S., and Liu, Y. (2022). Gelatin hydrolysates from sliver carp (*Hypophthalmichthys molitrix*) improve the antioxidant and cryoprotective properties of unwashed frozen fish mince. *Int. J. Food Sci. Technol.* 57, 2619–2627. doi: 10.1111/ijfs.15121

Zheng, L., Liu, J., Liu, R., Xing, Y., and Jiang, H. (2021). 3D printing performance of gels from wheat starch, flour and whole meal. *Food Chem.* 356:129546. doi: 10.1016/j.foodchem.2021.129546